Digest Journal of Nanomaterials and Biostructures Vol. 13, No. 1, January - March 2018, p. 177 - 183

SYNTHESIS OF VISIBLE-LIGHT-DRIVEN F-DOPED BiOI FOR PHOTODEGRADATION OF RHODAMINE B DYE

P. INTAPHONG[a], A. PHURUANGRAT[a,*], S. THONGTEM[b], T. THONGTEM[c,d]
[a]*Department of Materials Science and Technology, Faculty of Science, Prince of Songkla University, Hat Yai, Songkhla 90112, Thailand*
[b]*Department of Physics and Materials Science, Faculty of Science, Chiang Mai University, Chiang Mai 50200, Thailand*
[c]*Materials Science Research Center, Faculty of Science, Chiang Mai University, Chiang Mai 50200, Thailand*
[d]*Department of Chemistry, Faculty of Science, Chiang Mai University, Chiang Mai 50200, Thailand*

BiOI and F-doped BiOI photocatalysts were synthesized by a sonochemical method. X-ray diffraction (XRD), field emission scanning electron microscopy (FE-SEM), transmission electron microscopy (TEM), selected area electron diffraction (SAED) and X-ray photoelectron spectroscopy (XPS) clearly revealed the presence of BiOI nanoplates and F-doped BiOI nanobelts. Their photocatalytic activities were evaluated through the degradation of rhodamine B (RhB) activated by visible radiation. In this research, the 10 wt% F-doped BiOI photocatalyst has the highest decolorization efficiency of almost 100% within 180 min.

(Received November 1, 2017; Accepted January 28, 2018)

Keywords: F-doped BiOI; Nanobelts; Photocatalysis

1. Introduction

In the past decades, titanium dioxide (TiO_2) with a wide band gap of 3.2 eV has attracted intense interest used as a semiconducting photocatalyst for removal of hazardous organic pollutants containing in wastewater due to its chemical stability, non-toxicity and low cost [1–3]. Unfortunately, the application of TiO_2 has disadvantage to some degree because TiO_2 absorbs only UV radiation (4–5 % of solar light) [1, 4]. Thus, researchers focus to develop new visible-light-driven photocatalytic materials that can be activated by visible spectrum (≈ 43 % solar light) [1, 4].

BiOX (X = Cl, Br, I) as important V–VI–VII ternary compounds with unique $(Bi_2O_2)^{2+}$ layered structure and intergrown X^- layers, which have excellent photocatalytic performance for degradation of organic pollutants [5, 6]. They have been believed to be the promising photocatalysts. Bismuth (III) oxide iodide (BiOI) presents the highest photocatalytic activity under visible light irradiation. It is a unique layer structure and has excellent visible light absorbance [7, 8]. Its photocatalytic efficiency is greatly limited by high recombination rate of electron-hole pairs [5, 8, 9]. To improve the photocatalytic efficiency of BiOI, ionic dopants can lead to reduce the recombination rate of electrons and holes due to the presence of charge-trapping centers [10, 11].

In this study, F-doped BiOI photocatalyst was prepared by a simple and effective method called sonochemistry. Phase, morphology and photocatalytic properties were studied and discussed according to the experimental results. Effect of different contents of F dopant on photocatalytic performance was investigated through the degradation of rhodamine B (RhB) activated by visible radiation. A photocatalytic mechanism was also proposed and discussed.

*Corresponding author: phuruangrat@hotmail.com

2. Experiment

To synthesize BiOI, each 0.005 mole of $Bi(NO_3)_3 \cdot 6H_2O$ and NaI were dissolved in 100 ml deionized water under vigorous stirring until complete dissolution. Subsequently, 3 M NaOH was slowly added to the solution until pH of the solution was reached at 12. The solution was processed in 35 kHz ultrasonic bath at 80 ^oC for 5 h. In the end, precipitates were synthesized, collected and dried. Similarly, 1–10 wt% NaF were also added to each of the solutions and ultrasonically processed to form 1–10 wt% F-doped BiOI products.

Phase of the as-synthesized products was investigated by an X-ray diffractometer (XRD, Philips X'Pert MPD) with Cu K_α radiation operating at 30 kV and 0.02 $^o.s^{-1}$ scanning rate in the 2θ range of 10–60^o. Morphology and structure of the products were characterized by a field emission scanning electron microscope (FE-SEM, JEOL JSM-6335F) equipped with an energy dispersive X-ray spectrometer (EDX, Oxford instruments INCA system) operating at 35 kV and a transmission electron microscope (TEM, JEOL JEM-2010) operating at 200 kV. X-ray photoelectron spectroscopy (XPS) was carried out through a Kratos X-ray photoelectron spectrometer–Axis Ultra DLD with a monochromated Al K_α (1486.6 eV) radiation as an excitation source at 15 kV. All of spectra were calibrated with respect to 285.1 eV of C 1s electron peak.

To evaluate photocatalysis, each 200 mg catalyst was dispersed in 200 ml of $1x10^{-5}$ M RhB aqueous solution. The suspensions were kept in the dark for 30 min under magnetic stirring before xenon visible light illumination. At a given time interval, 5 ml solution was sampled and centrifuged. The residual concentration of RhB solution was measured at 553 nm by UV-visible spectroscopy (Perkin Elmer, Lambda 25). The decolorization efficiency was calculated by the equation

$$\text{Decolorization efficiency (\%)} = \frac{C_0 - C_t}{C_0} x100 \qquad (1)$$

, where C_0 is the initial concentration of RhB and C_t is the concentration of RhB after visible light irradiation within the elapsed time (t).

3. Results and discussion

Fig. 1 shows XRD patterns of the as-synthesized BiOI, 5 wt% F-doped BiOI and 10 wt% F-doped BiOI. In this research, the undoped product was indexed to the pure tetragonal BiOI phase of the JCPDS database no. 10-0445 [12].

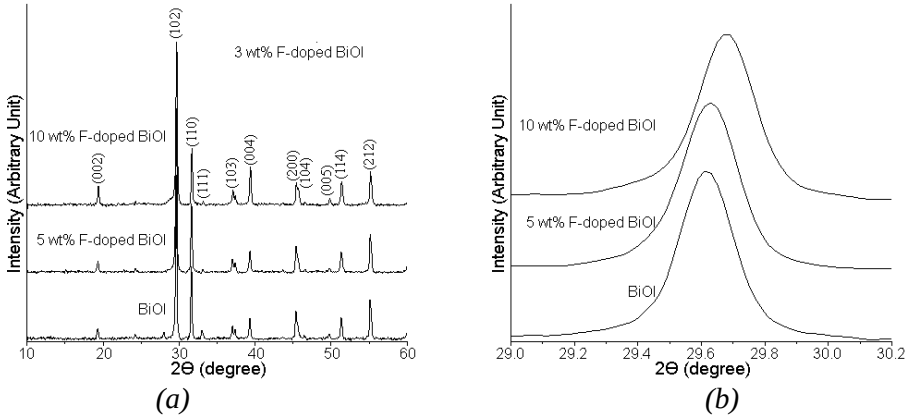

Fig. 1. XRD patterns of BiOI, 5 wt% F-doped BiOI and 10 wt% F-doped BiOI synthesized by sonochemical method for 2θ of (a) 10^o–60^o and (b) 29.0^o–30.2^o.

The diffraction peaks were at 2θ of 19.55°, 29.78°, 31.74°, 33.15°, 37.21°, 39.45°, 45.75°, 45.76°, 49.96°, 51.36° and 55.15° corresponding with the (002), (102), (110), (111), (103), (004), (200), (104), (005), (114) and (212) planes of tetragonal BiOI, respectively. For the 5 and 10 wt% F-doped BiOI samples, their XRD patterns were similar to that of pure tetragonal BiOI phase. They should be noted that the (102) plane of pure BiOI phase was gradually shifted to higher diffraction angle with the increase of doping concentration because the radius of F^- (0.133 nm) [10, 13] is smaller than that of I^- (0.216 nm) [14, 15]. The peak-shift indicates that F^- ions of the doped samples were incorporated into the BiOI lattice.

The XPS spectra of 10 wt% F-doped BiOI (Fig. 2) certified the presence of Bi, O, I and F containing in the sample. The high resolution XPS scan of Bi 4f shows two Bi $4f_{7/2}$ and Bi $4f_{5/2}$ peaks at 159.20 eV and 164.52 eV, certifying the presence of Bi^{3+} containing in 10 wt% F-doped BiOI crystal lattice [5, 8, 10]. The O 1s peak of 10 wt% F-doped BiOI at 530.00 eV is attributed to Bi–O of BiOI lattice [5, 8]. Other O 1s peaks at 530.91 and 532.57 eV were assigned to oxygen bonds of hydroxyl groups, moisture and contaminated oxide of carbon from ambient atmosphere [5, 8, 16]. The high resolution of I 3d XPS spectrum shows two peaks centered at 619.3 and 630.8 eV corresponding to the I $3d_{5/2}$ and I $3d_{3/2}$ peaks of I^- in BiOI lattice [5, 8], respectively. The 683.1 eV peak is a typical binding energy of the F 1s peak [10, 17].

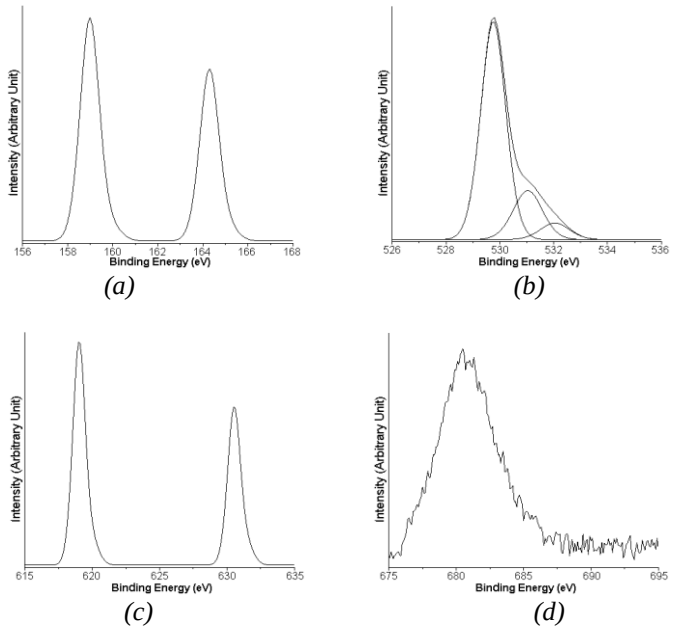

Fig. 2 XPS spectra of (a) Bi 4f, (b) O 1s, (c) I 3d and (d) F 1s of 10 wt% F-doped BiOI synthesized by sonochemical method.

The SEM was used to investigate the morphology of the as-synthesized BiOI and F-doped BiOI as the results shown in Fig. 3. SEM image of pure BiOI shows that the sample appears as irregular uniform nanoplates with edge length of 300–800 nm and thickness of 50 nm. The surfaces of BiOI nanoplates are very clear and smooth. Upon modification of the BiOI product by doping with F to form 1 wt% F-doped BiOI, the nanobelts were detected. SEM images of 5 and 10 wt% F-doped BiOI revealed that the products were consisted of a large number of uniform nanobelts orientated in different directions. For the 10 wt% F-doped BiOI nanobelts, they are 5–12 μm long and 30 nm wide. Previously, a one-dimensional nanosemiconductor shows higher photocatalytic performance than any other morphologies, caused by rapid electronic diffusion which can lead to reduce the recombination rate of photogenerated electrons and holes during photocatalysis [18, 19]. Possibly, F-doped BiOI nanobelts promoted the photocatalytic reaction rate. EDX of 10 wt% F-doped BiOI (not shown here) certified the presence of F, Bi, O and I, including Cu of a stub.

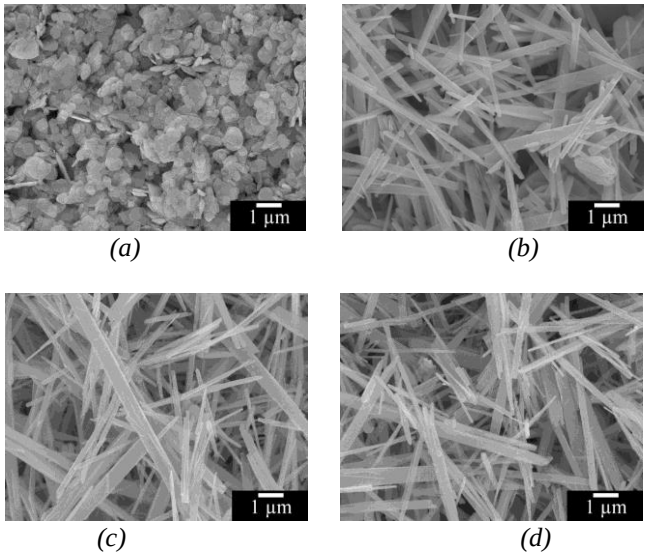

Fig. 3 SEM images of (a) BiOI, (b) 1 wt% F-doped BiOI, (c) 5 wt% F-doped BiOI and (d) 10 wt% F-doped BiOI synthesized by sonochemical method.

TEM images and SAED patterns of BiOI, 5 wt% F-doped BiOI and 10 wt% F-doped BiOI are shown in Fig. 4. The as-synthesized BiOI sample was composed of nanoplates. The SAED pattern can be specified as the (110), (200) and (1–10) planes with zone axis along the [00–1] direction of tetragonal BiOI structure. The top and bottom facets of the BiOI nanoplate are the (001) plane and the side facets are (110) plane. Upon doping with F^-, the morphology of the product changes from nanoplates to nanobelts. TEM images of 5 and 10 wt% F-doped BiOI show uniform nanobelts with very smooth surfaces. Their SAED patterns were recorded normal to the growth direction of each of a single nanobelt which was specified as the (110), (200) and (1–10) planes of tetragonal BiOI structure. They were suggested to be the F-doped BiOI nanobelts growing along the xy plane.

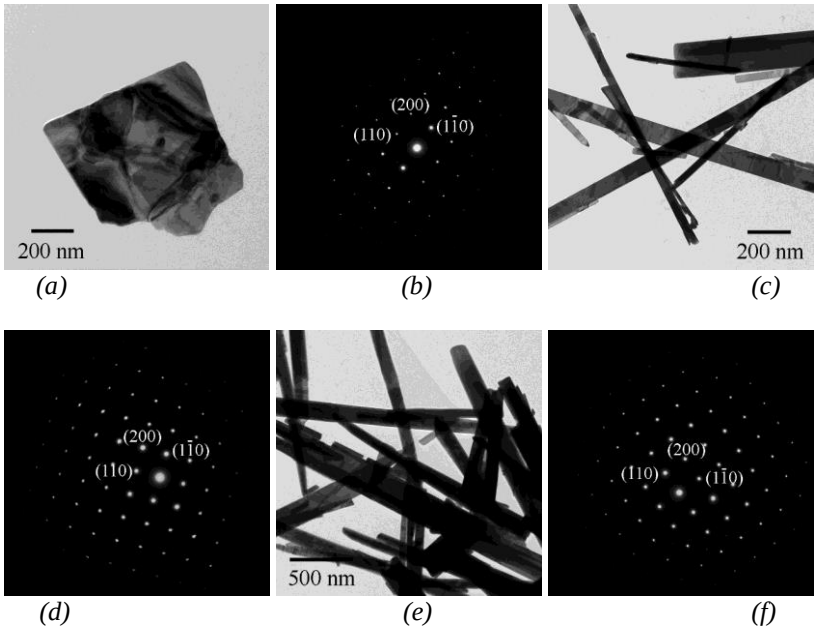

Fig. 4 TEM images and SAED patterns of (a, b) BiOI, (c, d) 5 wt% F-doped BiOI and (e, f) 10 wt% F-doped BiOI synthesized by sonochemical method.

Fig. 5a shows the temporal evolution of absorbance during the photodegradation of RhB by 10 wt% F-doped BiOI activated by visible radiation. The photocatalysis shows that the absorption peak at 553 nm wavelength gradually decreased with increasing in the length of irradiation time and shifted towards the blue region from 553 nm to 498 nm with the formation of deethylated RhB molecules within 180 min [20, 21]. Fig. 5b shows the decolorization efficiency of BiOI with and without F^- dopant under visible light irradiation. In this research, the photocatalytic efficiency of pure BiOI nanoplates was almost 81.19 %. The decolorization efficiency was increased by F^- doping modification. The photocatalytic activity of F-doped BiOI is obviously improved which is related to F^- dopant in the BiOI sample. Upon increasing the content of F^- dopant from 0 to 10 wt%, the efficiency for degradation of RhB was increased to almost 100 % within 180 min under visible light irradiation. Fig. 5c shows the reaction profiles of pure BiOI, 3 wt% F-doped BiOI, 5 wt% F-doped BiOI and 10 wt% F-doped BiOI photocatalysts proposed by Langmuir–Hinshelwood by the following equation

$$-\frac{dC_t}{dt} = \frac{K k_{TC} C_t}{1 + k_{TC} C_0} \qquad (2)$$

K is the Langmuir–Hinshelwood adsorption coefficient, and k_{TC} is the reaction rate constant [1]. If the initial concentration is sufficiently low, simplification of the reaction rate to a pseudo first-order equation is frequently given as follows

$$\ln \frac{C_0}{C_t} = k_{app} t \qquad (3)$$

, where k_{app} is the pseudo-first-order apparent rate constant (min^{-1}) [10, 14]. All reactions followed the pseudo-first-order rate constant indicated by slopes of the reaction profiles [20, 21]. Calculated rate constant and half-life ($t_{1/2}$) were 8.98×10^{-3} min^{-1} and 77.17 min for BiOI, 9.95×10^{-3} min^{-1} and 69.64 min for 3 wt% F-doped BiOI, 0.013 min^{-1} and 53.30 min for 5 wt% F-doped BiOI, and 0.020 min^{-1} and 34.65 min for 10 wt% F-doped BiOI. The results clearly demonstrated that 10 wt% F-doped BiOI nanobelts show the highest photocatalytic rate for the degradation of RhB dye solution activated by visible radiation.

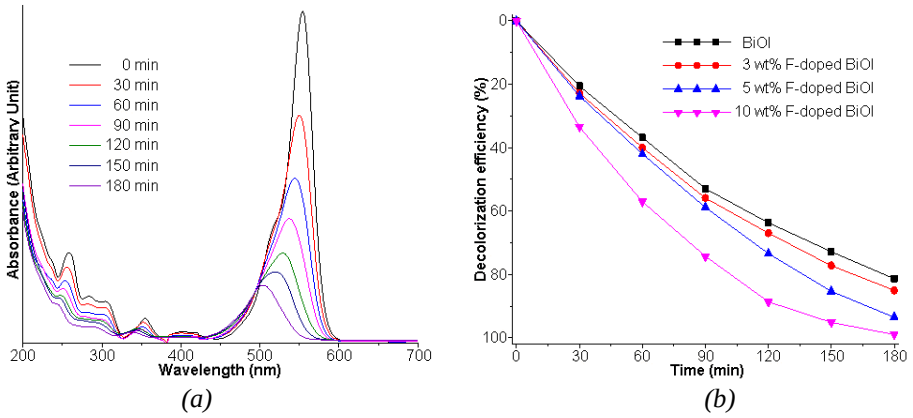

Fig. 5 (a) Absorbance of RhB solution photocatalyzed by 10 wt% F-doped BiOI. (b) Decolorization efficiency of BiOI, 3 wt% F-doped BiOI, 5 wt% F-doped BiOI and 10 wt% F-doped BiOI for different lengths of time activated by visible radiation.

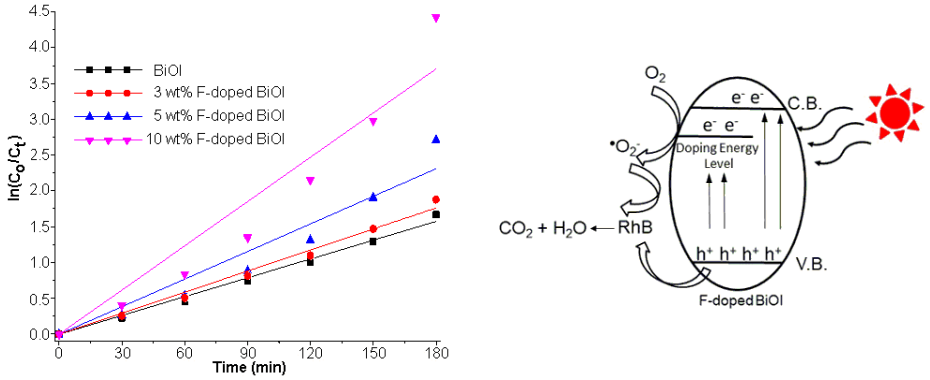

(c) *(d)*

Fig. 5 c) ln(C_0/C_t) plot of BiOI, 3 wt% F-doped BiOI, 5 wt% F-doped BiOI and 10 wt% F-doped BiOI for different lengths of time activated by visible radiation. (d) Schematic illustration of photocatalytic mechanism of F-doped BiOI.

Fig. 5d shows a schematic illustration for photocatalytic mechanism of F-doped BiOI. When F-doped BiOI nanobelts were activated by visible light, the electrons in valence band were excited to conduction band and doping energy level [22]. Further, the photoinduced positive holes oxidized RhB, while the excited electrons in the conduction band and doping energy level were rapidly trapped by molecular oxygen to form superoxide anionic radicals ($^{\bullet}O_2^-$). In the end, the degraded RhB molecules were transformed into CO_2 and H_2O. Thus, F dopant played an important role in the separation of photogenerated electrons and holes to improve the photocatalytic rate under visible light [5, 9, 22].

4. Conclusions

In summary, 0–10 wt% F-doped BiOI photocatalysts were synthesized by the sonochemical method and were evaluated for photodegradation of RhB under visible radiation. The 10 wt% F-doped BiOI sample was able to degrade RhB dye of ~100 % within 180 min.

Acknowledgment

We wish to thank the Thailand's Office of the Higher Education Commission for providing financial support through the Research Professional Development Project under the Science Achievement Scholarship of Thailand (SAST).

References

[1] P. Nualkaew, A. Phuruangrat, B. Kuntalue, P. Dumrongrojthanath, T. Thongtem, S. Thongtem, Russian J. Inorg. Chem. 62, 836 (2017).
[2] T. Arshad, S.A. Khan, M. Faisal, Z. Shah, K. Akhtar, A.M. Asiri, A.A. Ismail, B.G. Alhogbi, S. Bahadar, J. Mol. Liquids 241, 20 (2017).
[3] M. Sun, Q. Yan, Y. Shao, C. Wang, T. Yan, P. Ji, B. Du, Appl. Surf. Sci. 416, 288 (2017).
[4] T. Huang, W. Chen, T.Y. Liu, Q.L. Hao, X.H. Liu, Inter. J. Hydro. Energy 42, 12254 (2017).
[5] J. Xu, Y. Hu, C. Zeng, Y. Zhang, H. Huang, J. Colloid Interf. Sci. 505, 719 (2017).
[6] X. Qin, H. Cheng, W. Wan, B. Huang, X. Zhang, Y. Dai, Mater. Lett. 100, 285 (2013).
[7] W.W. Dai, Z.Y. Zhao, Mater. Chem. Phys. 193, 164 (2017).
[8] Y. Zhang, S.J. Park, J. Solid State Chem. 253, 421 (2017).
[9] Q. Yang, J. Huang, J. Zhong, J. Chen, J. Li, S. Sun, Curr. Appl. Phys. 17, 1202 (2017).

[10] S. Zhang, D. Wang, L. Song, Mater. Chem. Phys. 173, 298 (2016).
[11] E.M. Samsudin, S.B.A. Hamid, J.C. Juan, W.J. Basirun, G. Centi, Appl. Surf. Sci. 370, 380 (2016).
[12] Powder Diffract. File, JCPDS-ICDD, 12 Campus Bld., Newtown Square, PA 19073-3273, U.S.A., (2001).
[13] L. Samek, J. Mater. Sci. 30, 5649 (1995).
[14] X. Xiao, M. Lu, J. Nan, X. Zuo, W. Zhang, S. Liu, S. Wang, Appl. Catal. B 218, 398 (2017).
[15] Y.L. Su, Y.T. Xiao, Y.X. Du, S. Fu, Chinese Sci. Bull. 55, 2136 (2010).
[16] A. Phuruangrat, A. Maneechote, P. Dumrongrojthanath, N. Ekthammathat, S. Thongtem, T. Thongtem, Mater. Lett. 159, 289 (2015).
[17] Z. Pan, Y. Xiao, X. Tian, S. Wu, C. Chen, J. Deng, C. Xiao, G. Hu, Z. Wei, Mater. Sci. Semicond. Process. 17, 162 (2014).
[18] X. Ge, K. Hong, J. Zhang, L. Liu, M. Xu, Mater. Lett. 139, 119 (2015).
[19] M.W. Kadi, D. McKinney, R.M. Mohamed, I.A. Mkhalid, W. Sigmund, Ceram. Inter. 42, 4672 (2016).
[20] S. Jonjana, A. Phuruangrat, S. Thongtem, T. Thongtem, Mater. Lett. 179, 162 (2016).
[21] A. Phuruangrat, S. Putdum, P. Dumrongrojthanath, N. Ekthammathat, S. Thongtem, T. Thongtem, Mater. Sci. Semicond. Process. 34, 175 (2015).
[22] H. Li, Z. Yang, J. Zhang, Y. Huang, H. Ji, Y. Tong, Appl. Surf. Sci. 423, 1188 (2017).